A BILATERAL ANALOG FET OPTOCOUPLER

Robert I-Chih Chen
Tektronix, Inc.
Beaverton, Oregon 97077

William H. Sahm III
General Electric Co.
Auburn, New York 13021

I. INTRODUCTION

Recently, optoelectronic switches for low-level applications were described by Bussolati (1) and Brown (2). The optoelectronic switch proposed in Bussolati's paper consists of two phototransistors (PT) connected back-to-back with separate infrared emitting diodes (IRED's). Although by varying the ratio of the currents in the IRED's the offset voltage of the switch can then be zeroed, it is not a very practical device to use. An excellent performance, but technically complex and relatively costly hybrid to perform the same circuit function is detailed in Brown's paper. It is the purpose of this paper to present a new device called an optically-coupled bilateral analog FET, which is an economically advantageous design with technical trade-offs compared to the previous devices. This new device features a monolithic detector, coupled to an IRED, and is newly available in sample quantities. It provides the function of an ideal bilateral analog FET with isolated current control of the output conductance. This provides the advantage of optical isolation to the analog electronic functions of a linear, electronically variable, resistor (from 20 ohms to hundreds of megohms) and a fast bilateral ac low-level signal switch. The IRED and the detector are enclosed in a 6-pin DIP, although other configurations are possible. The structure and characteristics of this device are described in this paper. Possible applications, as well as limitations, are thoroughly analyzed.

II. DEVICE DESCRIPTION

a) Basic

The bilateral analog FET optocoupler consists of a symmetrical, bidirectional silicon detector chip, which provides the characteristics of a bidirectional FET when illuminated, closely coupled to an infrared emitting GaAs diode source (3). The resulting photoncoupled isolator provides an output conductance which is linear at low signal levels. The value of conductance is electrically controlled by the magnitude of an isolated current over a range of from a few nanomhos to a few millimhos. The stability of conductance is excellent, as expected from a silicon device. At higher bias levels the output device current saturates at a value roughly proportional to the IRED current and remains relatively constant out to the breakdown voltage of about 30V. As the shunt capacitance of the detector is low (≈10 pF) and the VI characteristics exhibit a very small offset voltage at zero current, the detector can be viewed as a remotely variable current controlled resistor from a circuit design viewpoint.

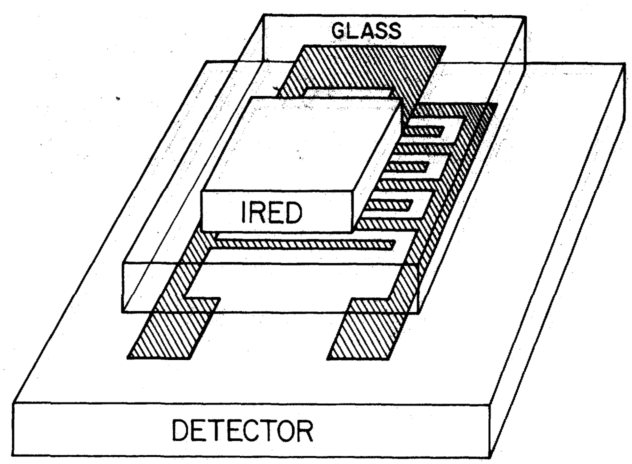

FIG. 1 Bilateral Analog FET Optocoupler Construction.

Received June 24, 1978

0098-3063/78/0300-0247$00.75©1978 IEEE

The construction of this optocoupler utilizes the superior glass dielectric "sandwich" in the rugged dual inline plastic package which has proven reliable across the General Electric optocoupler family. This is illustrated in Figure 1. The use of glass dielectric assures proper alignment and spacing of the emitter and detector, as well as providing excellent isolation of the input and output. The IRED is placed directly over the light sensitive portions of the detector chip to provide even illumination and minimize offset voltage and asymmetry of conductance. The close spacing maximizes light coupling efficiency to provide high conductance when the IRED is on.

b) Electrical Characteristics

To provide a quantitative perspective of the output and transfer characteristics of this optocoupler, Figures 2 and 3 plot the output V-I curves. This gives graphic illustration to the linear and saturated regions of operation.

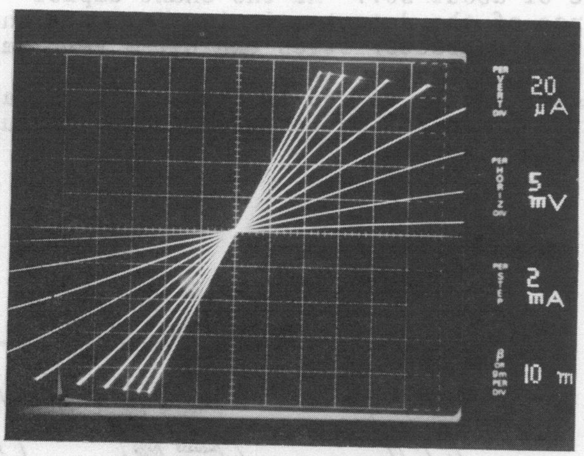

FIG. 2 Typical Low Level Output Characteristic.

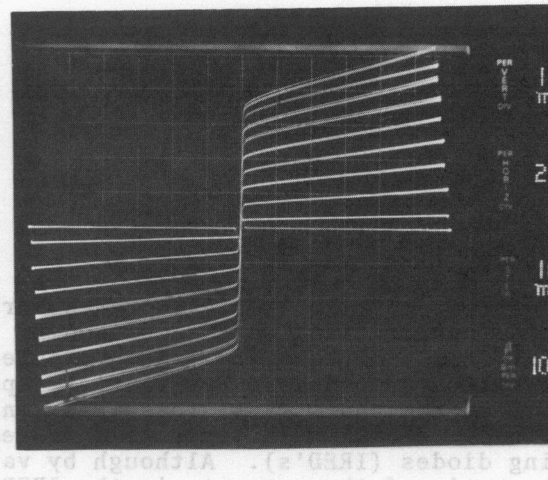

FIG. 3 Typical High Level Output.

Figure 4 plots the slope (resistance) of the low-level characteristic, at zero d.c. bias, vs. input current to the IRED. At lower input currents than these shown, the resistance rises rapidly to the over 300MΩ off-state value, while at higher, pulsed input currents the resistance can approach 10Ω on some units. Due to the IRED loss

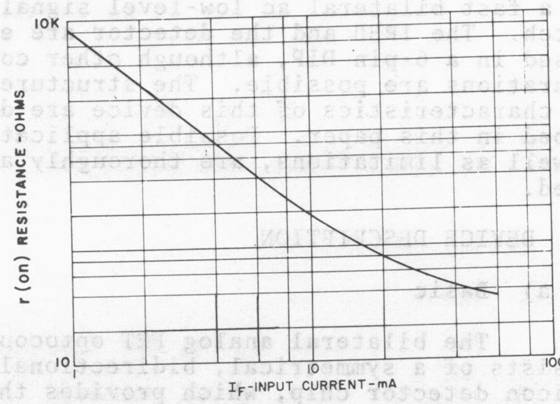

FIG. 4 Typical Resistance vs. Input Current.

in efficiency at low currents, most devices do not exhibit a lowering in resistance until 30 to 60 μA flows in the IRED. The signal level which will remain within the linear portion of the V-I curve is dependent on the bias point. This is illustrated in Figure 5, plotting maximum signal level vs. detector resistance, and Figure 6, which shows the maximum thevenin source voltage vs. the thevenin equivalent source impedance. The off-state resistance, with the IRED off, is dominated by leakage currents in the silicon junctions, as illustrated in Figure 7. The off-state impedance is therefore dominated by the roughly 10 pF of output shunt capacitance at most frequencies and moderate temperatures. The offset voltage is of low enough level to allow the device to be used with most sensors and operational amplifiers without compromising system performance, as illustrated in Figure 8.

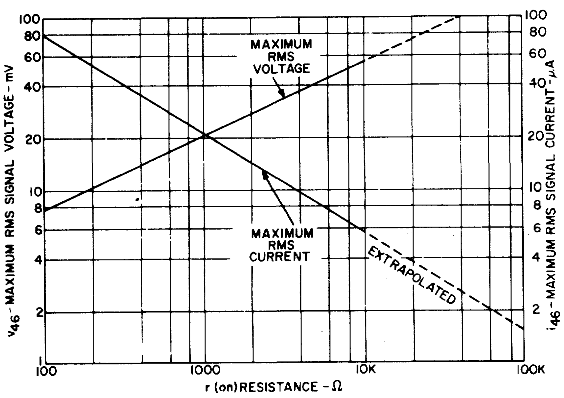

FIG. 5 Region of Linear Resistance.

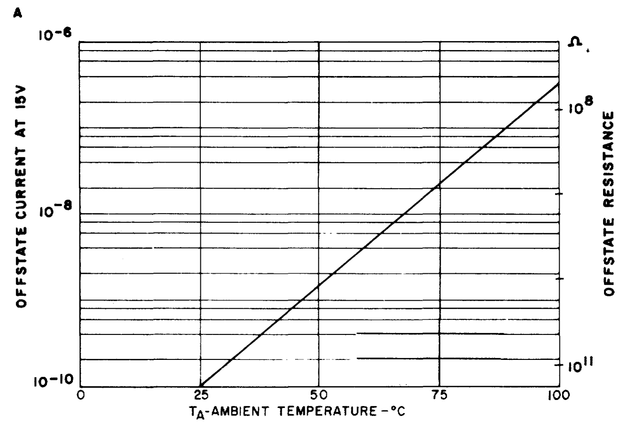

FIG. 7 Typical Off-state Current vs. Temperature.

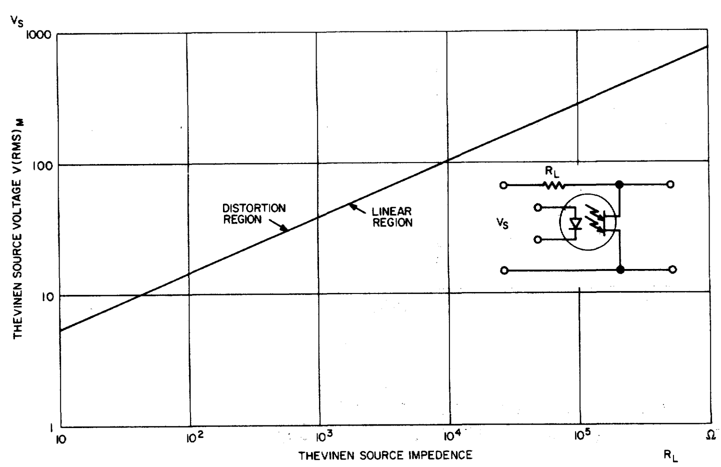

FIG. 6 Region of Linear Operation.

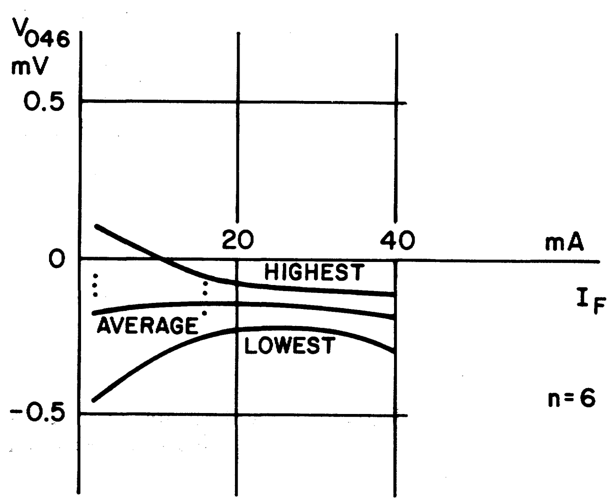

FIG. 8 Offset Voltage vs. Input Current.

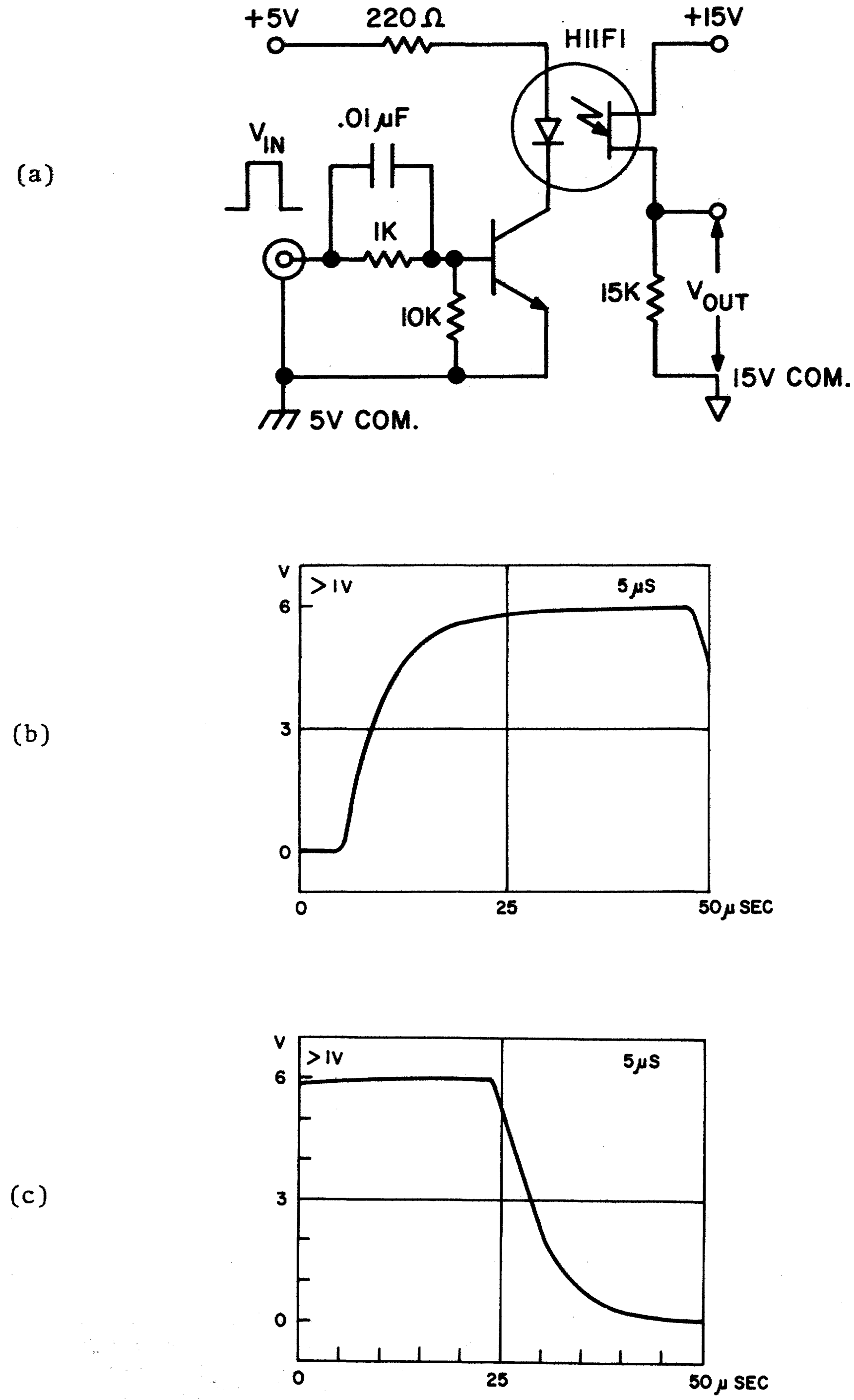

FIG. 9 Switching Characteristics as an Analog Switch.
(a) Measurement Circuits, (b & c) Output Waveforms.

(a)

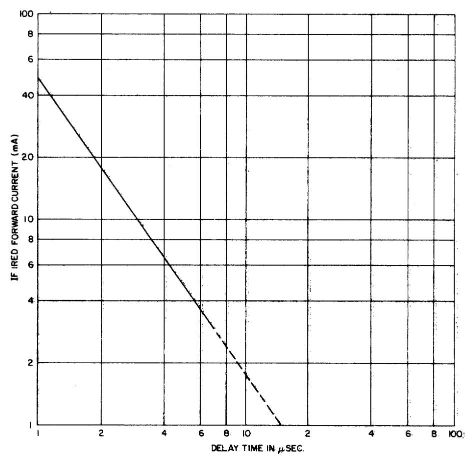

(b)

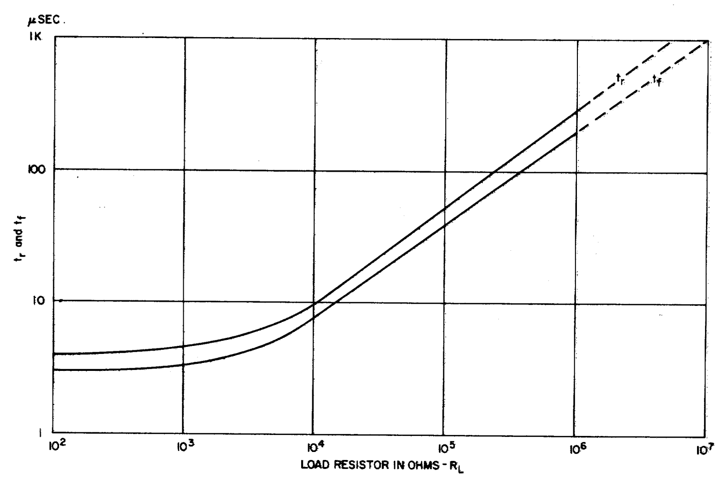

FIG. 10 Nonsaturated Switching Speeds.

The switching speed of the device is determined by internal capacitances, the availability of photon generated charges, and the time constant of the output impedance with its shunt capacitance and the equivalent Miller effect gain. Figure 9 illustrates a typical switching circuit and the resulting waveforms, while Figure 10 illustrates the effects of bias currents and impedances on switching speeds. Note that the times given by Figure 10 (b) plot exponential waveforms that are better described by time constants, and in saturated switching the turn-on exponential is truncated by saturation. These effects, in most circuits, combine to make turn-on appear much faster than turn-off. The corresponding equations for nonsaturating switching show the ratio of voltage across the device during switching to its final value to be:

for turn-on $V_T/V_\infty = 1\text{-}e^{-[\tau \times 10^9/(5\,R_L + 1500)]}$

for turn-off $V_T/V_\infty = 1\text{-}e^{-[\tau \times 10^9/(6\,R_L + 1800)]}$

for load resistor values $R_L \geq 10\ \text{K}\Omega$.

The turn-on waveform is truncated when the device bias point enters the linear region, while the turn-off waveform is relatively unaffected by saturation.

III. VARIABLE RESISTOR APPLICATIONS

Consumer electronics circuitry contains many functions which are based on the controllable attenuation of an analog signal. These applications are very common in audio and communications circuits. The most basic of these circuits is the simple voltage divider previously illustrated in Figure 6. This is easily extended to a remotely variable gain circuit, as illustrated in Figure 11. Note that the gain of the circuit is limited by the internal frequency compensation of the LM 307, i.e. operational amplifier gain bandwidth. The input voltage, V_{in}, must stay within the confines of Figure 5 to remain in the linear region.

Although wider bandwidth integrated amplifiers are available at additional cost, a conventional resistor attenuator was chosen to provide both wide bandwidth and high performance in the compression amplifier of Figure 12. This configuration provides an excellent compromise between minimum parts count and excellent performance, using 8 parts total to provide ± 3 db output, over a 54 db range of input signal, for signals from 300 Hz to 4400 Hz. Better performance can be obtained if the offset voltage of the operational amplifier is nulled, since it is the limiting factor that drives the H11F into the nonlinear region at high gains.

(a) Schematic.

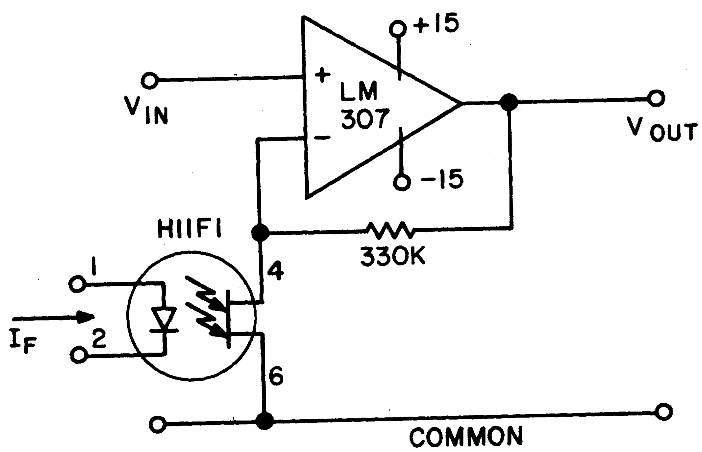

(b) Amplification vs. Control Current.

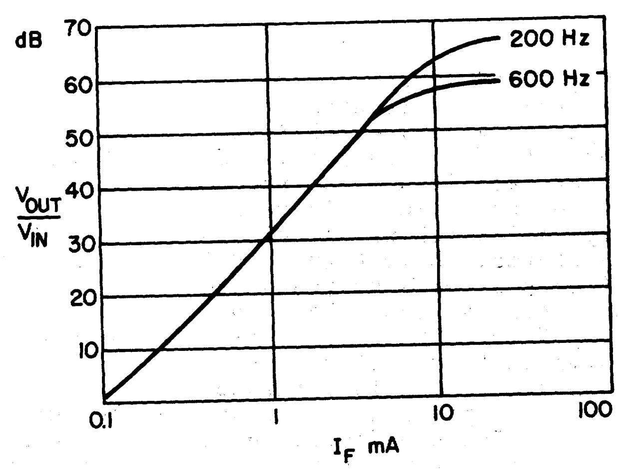

FIG. 11 Remotely Variable Gain Circuit.

(a) Test Circuit.

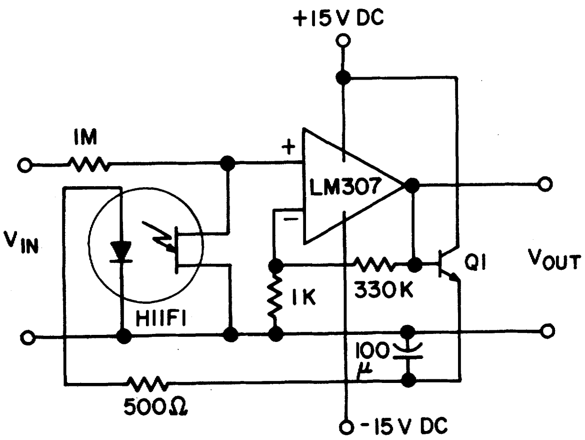

(b) Performance.

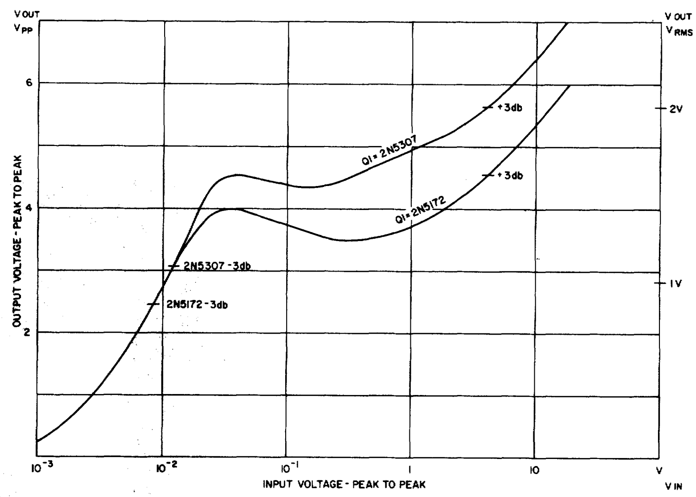

FIG. 12 Compression Amplifier.

Programmable, exponential attenuation of tone bursts or attack and decay of tones is a major factor in electronic music. The advent of the microcomputer has made it desirable to provide these features, while maintaining minimal cost. Straightforward D/A conversion of microprocessor output can be used in conjunction with the H11F to provide gain that is digitally controlled, via an algorithm stored in memory, using the circuit of Figure 11. To minimize computation complexity, memory and timing constraints, the use of hardwired attenuators can prove economical, from a systems viewpoint, under many circumstances. The simplest of these circuits, utilizing the H11F, provides an audio waveform envelope with a rapid rise to maximum amplitude, followed by an exponential decay back to zero. This type of waveform is typical of percussion and plucked string sounds. Figure 13 illustrates a simple circuit and illustrates the wave envelope resulting from the input of a 5V logic signal of longer duration than the envelope. As illustrated, a 20 mV RMS input of 1 KHz at 1 KΩ source impedance provided the tone input. A dynamic range of about 60 db was observed.

Programmable attacks and decays of waveform can be hardwired with somewhat more complexity, as illustrated in Figure 14, to simulate pipes, wind instruments, etc. This circuit requires an open collector logic input for proper operation, as illustrated, or the effect of the pull-

IEEE Transactions on Consumer Electronics, Vol. CE-24, No. 3, August 1978

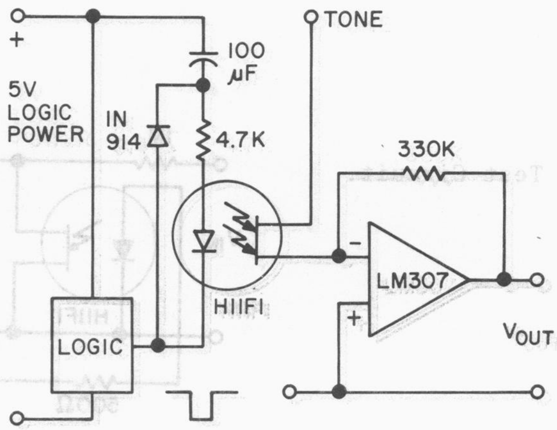

(a) Schematic.

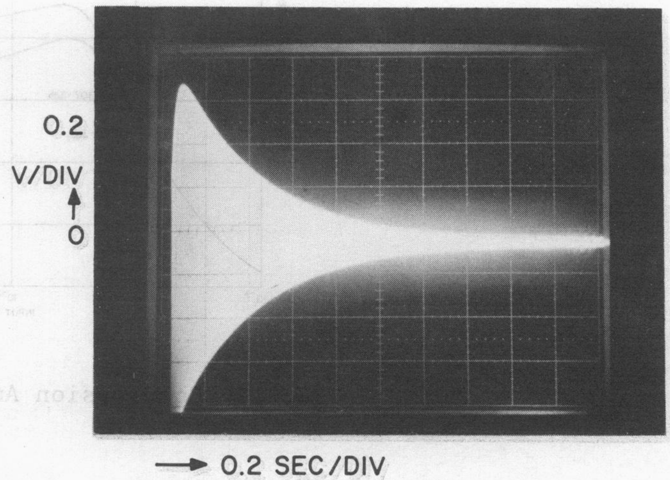

(b) 1 KHz Wave Envelope.

FIG. 13 Exponential Decay Attenuator - Percussion.

up resistor must be assessed in time constant calculations. The equations governing operation are:

for attack $15\ R2/(R2 + R3) \approx 0.38$ V,

for decay $R1 > 0.62\ R2$,

attack time constant $t_A \approx R1C$,

decay time constant $t_D \approx R1R2C/(R1-0.62\ R2)$.

As illustrated, R1=33KΩ, R2=18KΩ, R3=680KΩ, and C=8 μF with a 150 Hz, 20 mV RMS input at 1KΩ source impedance, and the dynamic range is about 60 db.

In a similar manner, this device can perform a variable resistor function which:

- determines the signal ratios in an audio mixer,
- adjusts the feedback resistor value to fine tune a phase shift oscillator,
- adjusts the time constant of an active filter,

and other functions too numerous to mention.

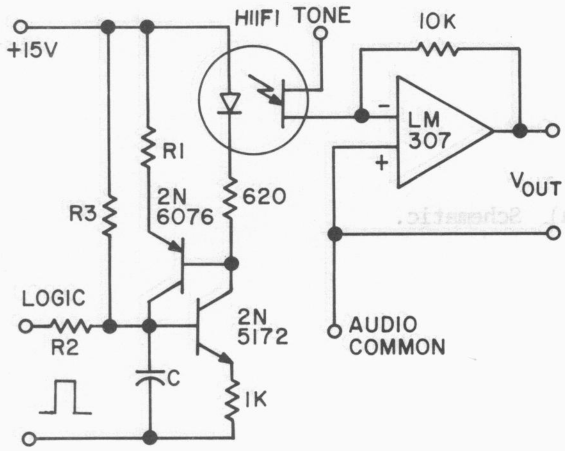

(a) Schematic.

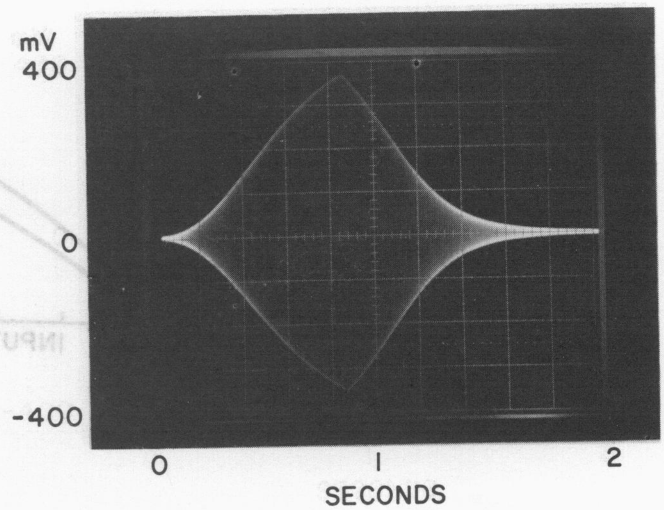

(b) 150 Hz Wave Envelope.

FIG. 14 Programmable Attack and Decay Attenuator - Pipes.

A power control circuit which provides a very simple remote phase control allows microprocessor or other low voltage control of incandescent lighting, small motors, heaters, etc. is illustrated in Figure 15. As illustrated, it provides phase angle turn-on pulses from 36° to 162° of the A.C. wave for currents in the IRED from 20 mA to 2 mA, respectively. The power control is off with no IRED current, I_F.

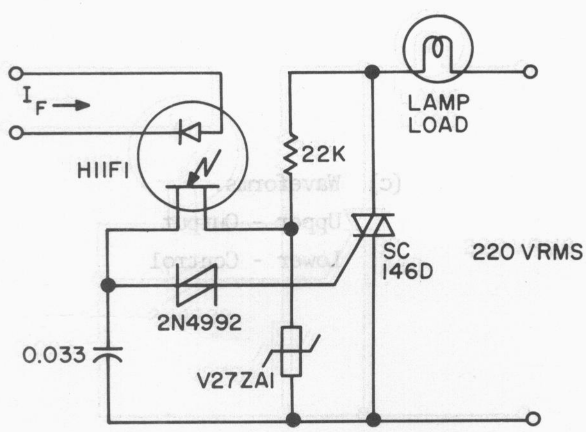

FIG. 15 Remote Control Lamp Dimmer Circuit.

(a) Schematic.

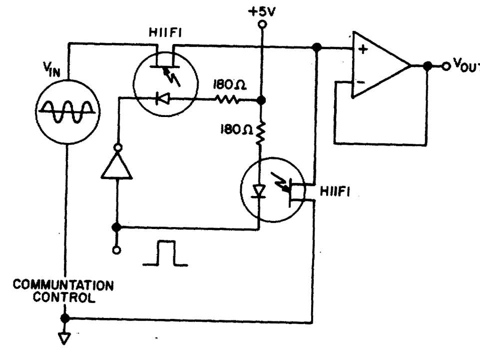

(b) Switching Time.

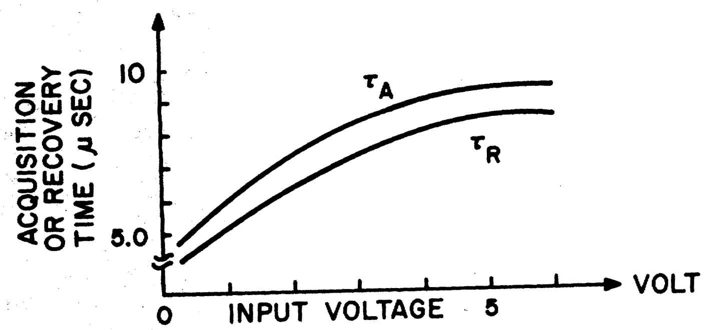

(c) Waveforms.
Upper - Output
Lower - Control

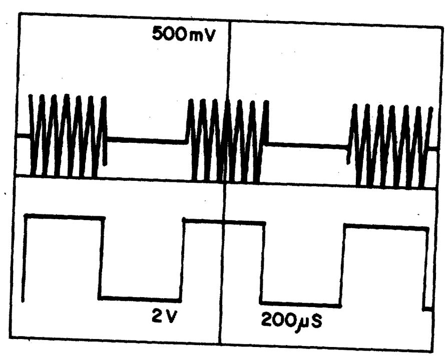

FIG. 16 Analog Commutator Circuit Performance.

IV. ANALOG SWITCH APPLICATIONS

The bilateral analog FET optocoupler can also be utilized as an isolated control analog switch, as will be illustrated in the next few examples. A series-parallel combination of the optocouplers can be utilized as an analog commutator. Figure 16 (a) shows the analog commutator configuration which is quite similar to the one suggested by Bussolati (1). A FET high input impedance op-amp connected as a unity-gain follower serves as a buffer between the signal source and the load. The switches can be viewed as a combination of two series-connected variable resistors in parallel with the input signal source. The input of the op-amp is tied to an equivalent voltage-divider network. If we use R_{on}=3KΩ and R_{off}=300MΩ, the variation of the voltage dividing ratio is from 0.00001 to 0.99999 which implies the error due to the opto-bilateral switches is about 0.001%. Because the switching speed of the opto-coupled bilateral switch (0% and 100% signal levels) is less than 50 μsec, this analog commutator works accurately for repetition rates below 20 KHz. For 200 mV dc input signal, the analog commutator has a rise time (0% to 99%) of about 5 μsec and a fall time (99% to 0%) of about 4 μsec. The rise time (acquisition time, τ_A) and fall time (recovery time, τ_R) of the commutator with a source impedance of 3MΩ as a function of input voltage is plotted in Figure 16. For a certain input voltage, the inverse of ($\tau_A + \tau_R$) will determine the upper limit of the operating frequency range of the commutator, and approaches 50 KHz at high input voltages. Extension of this technique allows a four-channel analog multiplexer to be constructed by adding three more input and control channels.

As illustrated in Figure 17 (a), the multiplexer allows selection of any of the four signal sources via the address selection and enable pulse. Switching transients have been observed at the transition state of the control signal. These transients (about 500 nsec) are much shorter than the acquisition time and recovery time (several micro-seconds), and they do not affect the operation of this multiplexer. To illustrate the operation of this multiplexer, four different waveforms are fed into four input channels, then sequentially multiplexed. Different dc offset voltages are applied to each channel so that the signal associated with each channel can be clearly identified in the output waveform, as shown in Figure 17 (b). The cross-talk between adjacent channels at various frequencies has been analyzed, and degrades about 20 db per decade increase in frequency. With 100 KHz input signal, the adjacent channel rejection is about 62 db, increasing to 100 db at 1 KHz. This figure can be further reduced with careful circuit layout.

The extremely high ratio of "Dark Resistance" to "Light Resistance" (≈180 db) and the medium switching speed (about 10 μsec) of this device, make it well suited for some sample and hold applications. A sample and hold module using the optocoupler as switches has been analyzed. The circuit diagram is shown in Figure 18 (a). With the control signal "Low", SW1 and SW2 are in the low-impedance state, while SW3 is in the high-impedance state. The output of the unity-gain op-amp follows the input signal through SW1 and charges the capacitor through SW2. The circuit is in the "TRACK" or "SAMPLE" mode. When the control signal goes high, SW1 and SW2 are in the high-impedance state and SW3 is in the low-impedance state. The output voltage follows the voltage across the capacitor through SW3. Then the circuit is in the "HOLD" mode. Figure 18 (b) shows the Sample and Hold Circuit in operation. The upper trace is the control signal, while the middle and the lower traces are the input and the output signals, respectively.

To measure the aperture time of this S & H, the input signal starts a ramp the moment the control signal switches from "Low" to "High". The output signal will have a finite change, and the transition time corresponds to the S & H aperture time. The acquisition time proves to be a function of both the storage capacitance, C, and the change in input voltage. The droop rate is also a function of the storage capacitor and the change in input voltage. The plots of acquisition time versus Δ Vin and droop rate versus capacitance are given in Figures 18 (c) and 18 (d).

V. SUMMARY

An optoelectronic coupler, which is a combination of a GaAs IRED and a bilateral, linear, silicon detector, has been developed and is available in sample quantities. This device can replace a mechanical relay in small-signal application with much higher repetition rate. It also can function as a remotely variable current controlled resistor, replacing photo conductive cells (4) and conventional optocouplers.

The characteristics and construction of the device have been detailed. Typical applications, as both an analog switch and a remotely variable resistor, have been presented and the performance documented. Five linear and three analog switch applications are included.

(a) Schematic.

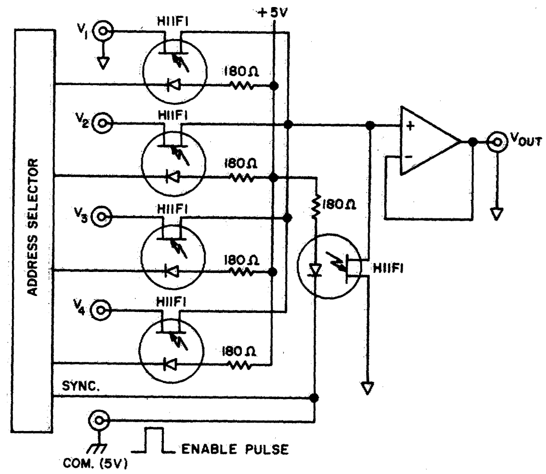

(b) Output Waveforms for Sequential Address.

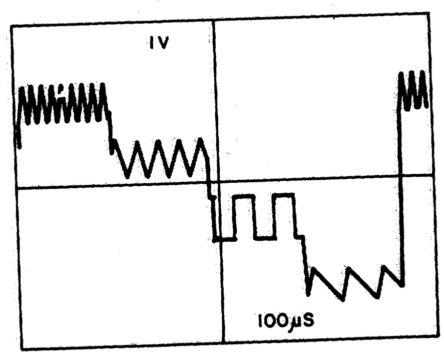

FIG. 17 Four Channel Multiplexer.

18

(a) Schematic.

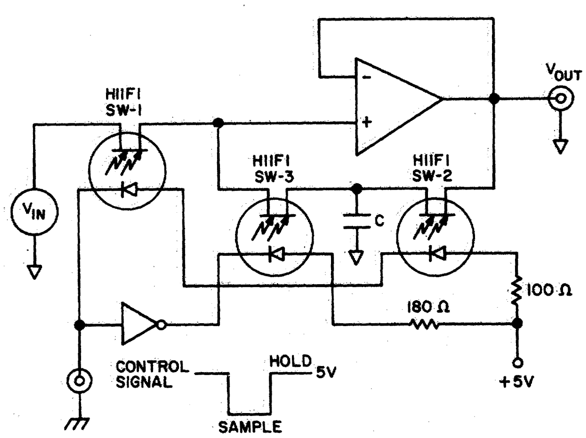

(b) Operation.
Upper-Control
5V/cm
Mid-Input
1V/cm
Lower-Output
1V/cm

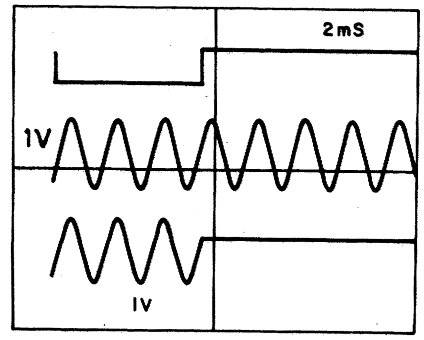

(c)

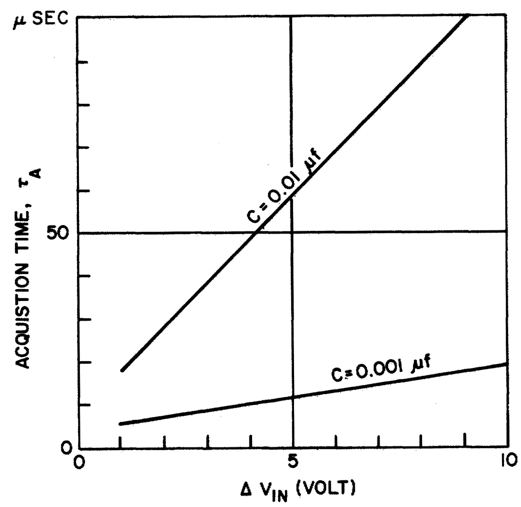

(d)

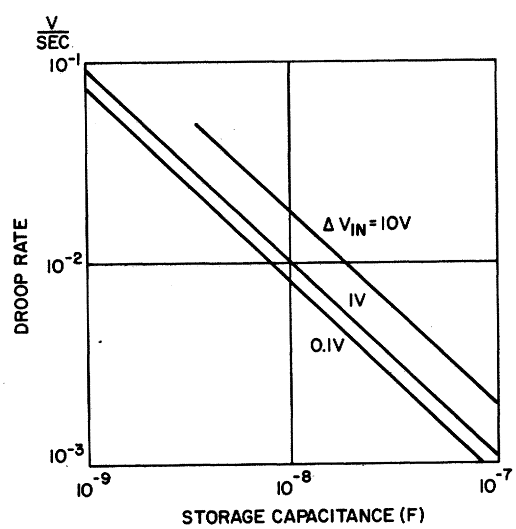

FIG. 18 Sample and Hold Module.

Further development of this device will depend on feedback from the marketplace. Possible performance gains could be made in:

- on-state resistance minimization,
- on-state resistance tolerance,
- switching speed,
- breakdown voltage,
- current transfer ratio,
- offset voltage,
- region of linearity.

Most of these improvements would require compromise of other parameters, although material advances (5) may eliminate or reduce the effect of some of these trade-offs.

VI. ACKNOWLEDGMENTS

The authors would like to express their thanks to the following people, for without their contributions this paper would not have been published:

D. K. Barney - Art Work
H. C. Chu - Device Processing
D. R. Grafham - Circuit Development
J. D. Harnden, Jr. - Circuit Concepts
A. LaValle - Circuit Characterization
J. Maurer - Manuscript
N. Patrick - Manuscript

VII. REFERENCES

1. Camillo Bussolati, Emilio C. Gatti, D. Marioli, P. F. Manfredi, "An Optoelectronic Switch for Low-Level Analog Applications", IEEE Trans. on Instrumentation and Measurement, Vol. IM-26, No. 2, June 1977.

2. D. M. Brown, M. Garfinkel, J. Laurent and P. A. McConnelee, "Solid State Relay", General Electric Technical Information Series, No. 78CRD040. Available from GE, CR&D, PO Box 43, B. 5, Schenectady, N. Y. 12301.

3. Robert I. Chen, Hing C. Chu, William H. Sahm, "A Remote Optically-Coupled Analog Switch". Patent Disclosure Letter, GE-Semiconductor Products Dept., June 10, 1977.

4. G. A. Imagee, "Development of Sandwich Structured Photosensitive Films for Application to Non-Contact Potentiometers", Naval Avionics Facility-NAF1-TR2148.

5. M. Abe, I. Umebu, O. Hasegawa, S. Tamakoshi, etc., "High-Efficiency, Long-Lived GaAlAs LED's for Fiber-Optical Communications". Proc. of the S.I.D., Vol. 18/2, Second Quarter 1977.

BIOGRAPHIES

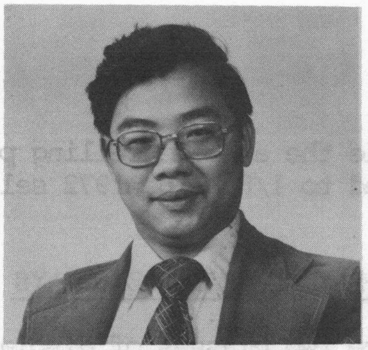

R. I-Chih Chen

Robert I-Chih Chen received his BSEE from National Taiwan Cheng Kung University, Tainan, Taiwan in 1970; the MSEE from South Dakota School of Mines and Technology, Rapid City, South Dakota, in 1973; and the Degree of Electrical Engineering from Syracuse University, Syracuse, N. Y. in 1977.

From 1973 through 1974, he was employed by Delco Electronics, Div. of General Motors at Kokomo, Indiana, where he undertook the project of developing and manufacturing the solid-state electronic ignition modules. In 1974 he joined the Semiconductor Products Dept. of General Electric Co. at Syracuse, N. Y. At G.E., he was responsible for the development of various new semiconductor products, especially in the optoelectronics area. Since September 1977 he has been the manager of the optoelectronic and passive component engineering department of Tektronix, Inc. at Portland, Oregon.

Mr. Chen is a member of Eta Kappa Nu, IEEE, ISHM, and SID.

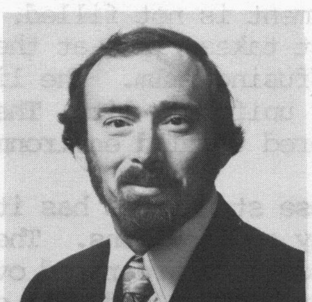

William H. Sahm

William H. Sahm III is a Consulting Application Engineer with General Electric Semiconductor at Auburn, N. Y. Bill has over sixteen years engineering experience, including assignments in the product evaluation, product design, test equipment design and application engineering areas. He has extensive experience in the device, circuit application, and systems design aspects of low current thyristors, metal oxide varistors, optoelectronics, transistors, triacs, tunnel diodes, and unijunctions. He is the author of the G.E. Optoelectronics Manual and numerous application notes, magazine articles and technical papers concerning these devices.

Bill is a member of Eta Kappa Nu, Tau Beta Pi and IEEE Electron Device Group. He is a licensed professional engineer in New York State and a 1964 graduate of Syracuse University.

Paper presented at the 19th Annual IEEE Chicago Spring Conference June 1978